

Generation of Optical Frequency Comb via Cross-Phase Modulation in an SOI Waveguide

Yuanfei Zhang, Honghui Zhang, and Chester Shu

Center for Advanced Research in Photonics, Department of Electronic Engineering, The Chinese University of Hong Kong, Shatin, N.T., Hong Kong

Author e-mail address: yfzhang@link.cuhk.edu.hk

Abstract: Using temporal Talbot processing followed by cross-phase modulation in a silicon-on-insulator waveguide, we experimentally multiply the repetition rate of a 10-GHz optical pulse train and generate widely spaced optical frequency combs up to 50 GHz. © 2021 The Author(s)

1. Introduction

Optical frequency combs with flexible spacings are attractive for use in next generation optical networks supporting flexible grid [1]. A frequency comb generator on silicon-on-insulator (SOI) is desirable to enable integration with other chip-based functionalities while reducing the power consumption and footprint of the whole system [2]. In this paper, we combine the temporal Talbot effect and cross-phase modulation (XPM) to realize the generation of optical frequency combs with wide spacing. The coherent comb source can provide multiple optical carriers to support high-speed data transmission [3-5]. In our approach, linear temporal Talbot effect is used to multiply the repetition rate of the incident optical pulse train. Following that, nonlinear XPM is applied to generate widely spaced optical frequency combs up to 50 GHz.

2. Principle and Experiment

2.1. Repetition Rate Multiplication Based on Temporal Talbot Effect

The fractional temporal Talbot effect is observed when a pulse train propagates along a dispersive element as shown in Fig. 1. Multiplication of the input pulse repetition rate with different factors is observed during the transmission when the distance z_m satisfies the following condition in the dispersion medium, $\beta_2 \cdot z_m = n \cdot T_0^2/m \cdot 2\pi$ [6]. Here, n/m is an irreducible fraction, and m is an integer larger than 1 ($m = 2, 3, \dots$). At the fractional Talbot distance z_m , a multiplied optical pulse train with a period of T_0/m can be observed and m is the multiplication factor. Thus, dispersive media with different dispersion values can be used to support variable multiplication factors. In other words, by changing the dispersion value or the length of the dispersive medium, the repetition rate multiplication factor can be adjusted. After the multiplier, the repetition rate of the optical pulses increases, while the amplitudes of the different spectral components remain unchanged by dispersion [8]. Previously, we have demonstrated the approach and experimentally performed pulse multiplication by a controllable factor of 3, 4, and 5, followed by optical frequency comb generation through the nonlinear XPM process [3, 4]. While our previous work was performed on the fiber platform, the comb generation approach based on XPM can also be realized on a silicon-based photonic integration platform as described in the following subsection.

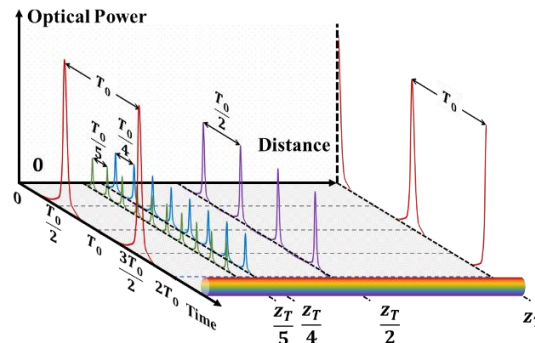


Fig. 1. Evolution of an optical pulse train during its propagation along a dispersive fiber. The period of the pulse train at the distance of 0, $z_0/5$, $z_0/4$, $z_0/2$ and z_0 is T_0 , $T_0/5$, $T_0/4$, $T_0/2$, and T_0 , respectively.

2.2. Design of Silicon Waveguide for Cross-Phase Modulation

The silicon waveguide was fabricated on the silicon platform by a commercial foundry. Electron beam lithography and reactive ion etching processes have been used to fabricate the device using a 220 nm thick silicon layer on top of

a 2 μm buried oxide layer with upper oxide cladding. The silicon strip waveguide has a total length of ~ 0.5 cm with a dimension of $450\text{ nm} \times 220\text{ nm}$. An FDTD mode solver (Lumerical Solution Inc.) is used to calculate the transverse electric-like (TE-like) guided optical mode and gives an effective modal area of approximately $0.12\ \mu\text{m}^2$ at a wavelength of 1550 nm . The corresponding nonlinear coefficient is $\sim 250/(\text{W}\cdot\text{m})$, while the dispersion is $\sim 2641\text{ ps}/(\text{nm}\cdot\text{km})$ with a dispersion slope of $\sim 4.7\text{ ps}/(\text{nm}^2\cdot\text{km})$ for the TE-like mode. The optical wave is coupled in and out of the waveguide through a pair of edge couplers. The propagation loss of the silicon waveguide is $\sim 1.5\text{ dB}/\text{cm}$ as measured by the cutback method while the total insertion loss including the fiber-device coupling is $\sim 5.8\text{ dB}$.

2.3. Experimental Setup

Figure 2 shows the experimental setup for the generation of optical frequency combs via XPM in an SOI waveguide. A continuous-wave laser (CW1) centered at 1550 nm is shaped into a 10-GHz optical pulse train via phase modulation and chirp compensation by a 2.1-km single-mode fiber (SMF). By further propagating through a 1-km HNLF followed by offset filtering, the optical pulse is reshaped to a pedestal-free pulse with a width of 2 ps . The pulses then propagate along different dispersive modules to initiate the temporal Talbot effect for repetition rate multiplication. Two sets of dispersive modules are applied, Module 1 and Module 2. Module 1 with a dispersion value of $\sim 370.4\text{ ps}/\text{nm}$ consists of 3.48-km dispersion-compensating fiber (DCF) and 530-m SMF, and Module 2 with a dispersion value of $\sim 298.6\text{ ps}/\text{nm}$ is composed of 3.02-km DCF and 530-m SMF. These two modules provide different total dispersion values. Consequently, the repetition rate of the multiplied optical pulse can be set at 40 GHz or 50 GHz . The rate-multiplied optical pulses are further amplified by an erbium-doped fiber amplifier (EDFA) and filtered by a tunable BPF to reduce the amplified spontaneous emission (ASE) noise. The amplified pulses serve as the XPM pump while another CW laser (CW2) at 1565 nm is employed as the probe wave. The pulsed pump and the CW probe are combined through a 3-dB coupler and co-propagate along the 0.5-cm silicon waveguide. The polarization states of the pump and probe are aligned to maximize the XPM effect. An optical spectrum analyzer (OSA) is used to observe the generated optical frequency combs.

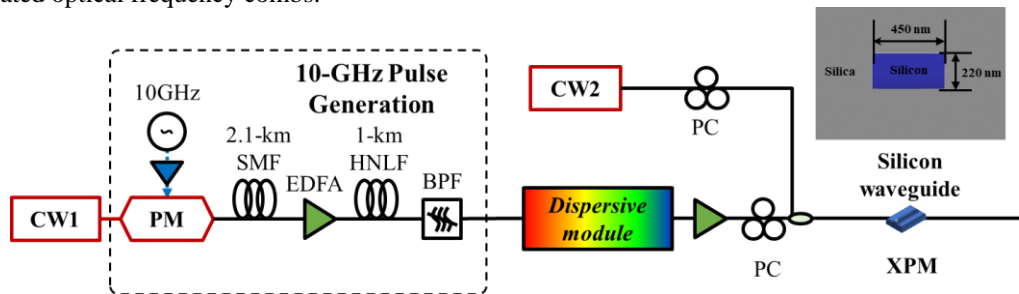


Fig. 2. Experimental setup for the generation of optical frequency combs via cross-phase modulation (XPM) in an SOI waveguide. Inset: Cross-section of the silicon strip waveguide with upper oxide cladding. CW: continuous-wave laser; PM: phase modulator; SMF: single-mode fiber; EDFA: erbium-doped fiber amplifier; HNLF: highly nonlinear fiber; BPF: band-pass filter; PC: polarization controller.

3. Results and Discussion

Figure 3 depicts the optical pulse trains in the time domain before and after the dispersive module, showing multiplication of the repetition rate by 4 and 5 times via Module 1 and Module 2, respectively. The input pulse trains and rate-multiplied pulses after different dispersive media are measured by a 500-GHz optical sampling oscilloscope. The rate-multiplied pulses have the same pulse widths (1.8 ps) as the input 10-GHz pulse. The pulse quality is not affected by the energy-efficient, phase-only temporal Talbot processing. The pulsed pump has an input average power of 20 dBm while the CW probe wave has an input power of 10 dBm . Consequently, multiple comb lines with a 10-GHz , 40-GHz , and 50-GHz frequency spacing are generated symmetrically around the original CW carrier as shown in Fig. 3. Since the phase modulation by XPM process is only sensitive to the intensity of the pulsed pump, the repetition rate determines the frequency spacing of the output comb. A relatively wide frequency comb is generated owing to the high peak power of the pulsed pump as well as the large nonlinear coefficient and flat dispersion profile of the silicon waveguide. The flat dispersion profile also gives rise to negligible group velocity dispersion and walk-off effect between the CW probe and the pulsed pump. Ideally, the maximum nonlinear phase induced by XPM is given by $\theta = 2\gamma PL$, where γ is the nonlinear coefficient of the waveguide, P is the peak power of the pump and L is the effective length of the silicon waveguide [7]. As shown in Fig. 4, the spectral profile of the generated 10-GHz , 40-GHz , and 50-GHz frequency combs span over a wavelength range of $\sim 14\text{ nm}$, $\sim 11.6\text{ nm}$, and $\sim 10.6\text{ nm}$, respectively. The maximum carrier-to-noise ratio (CNR) of the 40-GHz and 50-GHz frequency combs are measured to be 45.1 dB and 45.2 dB , respectively. The maximum CNR of the 10-GHz frequency comb in Fig. 3 (a) is larger than 20 dB while the exact value is not measurable due to the limited resolution of our OSA (0.02 nm). The maximum nonlinear phase

shift induced by 10-GHz, 40-GHz, and 50-GHz pulses are calculated to be $\sim 3.4\pi$, 0.86π and 0.68π , respectively. Optical frequency combs with larger spectral bandwidth can be realized through implementing stronger pump power of XPM. With higher pump power, the nonlinear loss in silicon caused by two-photon absorption and free-carrier absorption cannot be neglected but they can be suppressed significantly by introducing a reverse-biased p-i-n diode embedded in the silicon waveguide [8]. Our generated frequency combs can be used to supply coherent optical carriers at different wavelengths to support high-speed data modulation in a WDM communication system [4].

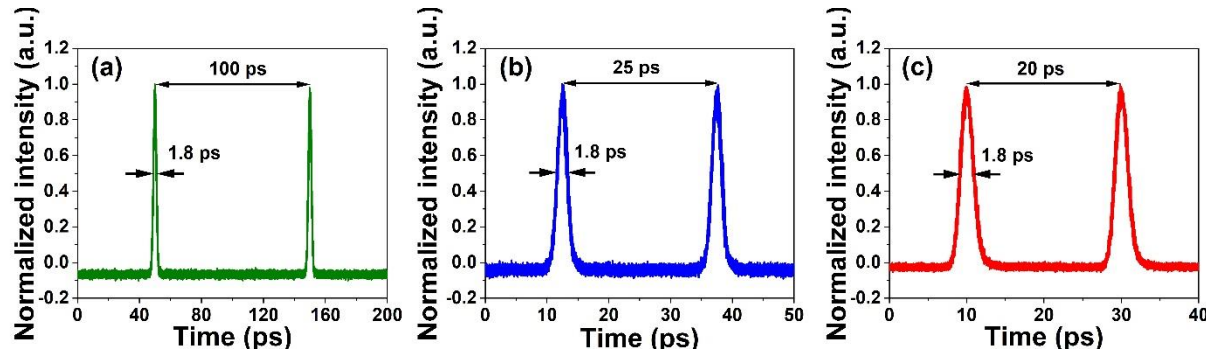


Fig. 3. Measured input and output optical pulse trains in different time scales. Input waveform at (a) 10 GHz and output waveforms at (b) 40 GHz, and (c) 50 GHz with multiplication factors of 4 and 5, respectively.

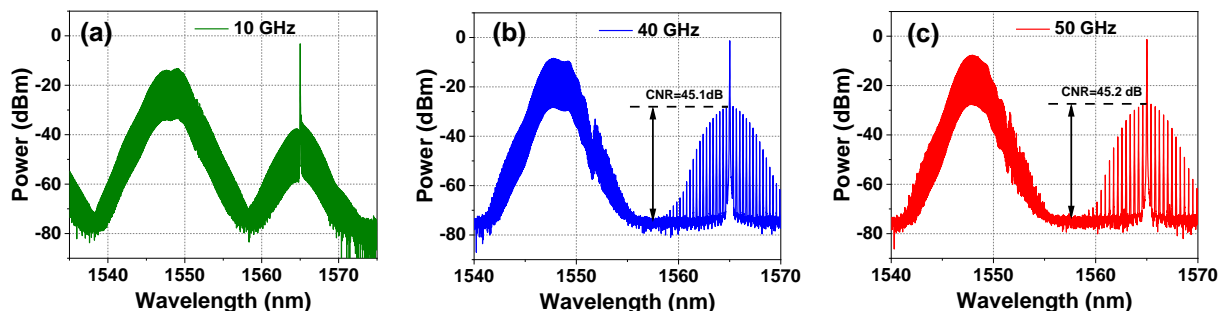


Fig. 4. Measurement results of the generated optical frequency combs after XPM on a silicon chip with a spacing of 10 GHz (a), 40 GHz (b), and 50 GHz (c) by an optical spectrum analyzer.

4. Conclusion

Using fractional temporal Talbot processing followed by XPM in an SOI waveguide, we have demonstrated the generation of coherent optical frequency combs up to 50 GHz spacing at the telecommunication band. A carrier-to-noise ratio of over 45 dB has been achieved in both the 40 GHz and 50 GHz frequency combs.

Acknowledgment

The authors thank Dr. Qijie Xie for the fruitful discussion. This work was supported by the Hong Kong RGC through GRF Grants 14209517, 14210419, and 14211120.

5. References

- [1] L. Romero Cortés, R. Maram, H. Guillet de Chatellus, and J. Azaña, *Laser Photonics Rev.* **13**, 1900176 (2019).
- [2] A. G. Griffith, R. K. Lau, J. Cardenas, Y. Okawachi, A. Mohanty, R. Fain, Y. H. Lee, M. Yu, C. T. Phare, C. B. Poitras, A. L. Gaeta, and M. Lipson, *Nat Commun* **6**, 6299 (2015).
- [3] Q. Xie, B. Zheng, and C. Shu, *IEEE Photonics Technol. Lett.* **30**, 975-978 (2018).
- [4] B. Zheng, Q. Xie, and C. Shu, *J. Lightwave Technol.* **36**, 2651-2659 (2018).
- [5] H. Zhang, Q. Xie, Q. Zhang, and C. Shu, *IEEE J. Sel. Top. Quantum Electron.* **27**, 1-6 (2021).
- [6] J. Azana, and M. A. Muriel, *IEEE J. Sel. Top. Quantum Electron.* **7**, 728-744 (2001).
- [7] M. Pelusi, H. Nguyen Tan, K. Solis-Trapala, T. Inoue, and S. Namiki, *IEEE J. Sel. Top. Quantum Electron.* **24**, 1-12 (2018).
- [8] H. Rong, R. Jones, A. Liu, O. Cohen, D. Hak, A. Fang, and M. Paniccia, *Nature* **433**, 725-728 (2005).